

Effects of CdCl₂ treatment on deep levels in CdTe and their implications on thin film solar cells: a comprehensive photoluminescence study

I. M. Dharmadasa¹ · O. K. Echendu¹ · F. Fauzi¹ · N. A. Abdul-Manaf¹ ·
H. I. Salim¹ · T. Druffel² · R. Dharmadasa² · B. Lavery²

Received: 5 March 2015 / Accepted: 18 April 2015 / Published online: 9 May 2015
© Springer Science+Business Media New York 2015

Abstract This work is aimed at studying defect level distributions in the bandgap of CdTe thin films, used for solar cell development. In particular, the effects of CdCl₂ treatment on the defect levels are the main objectives of this research. Four different nearly optimised CdTe thin films were electroplated using three different Cd-precursors (CdSO₄, Cd(NO₃)₂ and CdCl₂), and bulk CdTe wafers purchased from industry were studied using low temperature photoluminescence. The finger prints of defects, 0.55 eV below the conduction band down to the valence band edge were investigated. In all of the CdTe layers, four electron trap levels were observed with varying intensities but at very similar energy positions, indicating that the origin of these defects are mainly from native defects. CdCl₂ treatment and annealing eliminates two defect levels completely and the mid-gap recombination centres are reduced drastically by this processing step. The optical bandgap of all four as-deposited CdTe layers is ~1.50 eV, and reduces to ~1.47 eV after CdCl₂ treatment. The material grown using the CdCl₂ precursor seems to produce CdTe material with the cleanest bandgap, most probably due to the built-in CdCl₂ treatment while growing the material.

1 Introduction

Thin film solar cells based on CdS/CdTe structures have achieved 21.5 % efficiency to date, for small area, lab-scale solar cells [1]. The performance, reproducibility, yield, stability and lifetime of these solar cells depend on defect levels present in the materials and device structures. Therefore, a thorough knowledge of these defect levels is of paramount importance in the research, development and manufacturing of CdS/CdTe solar panels to achieve higher efficiencies.

The heat treatment of CdTe thin films in the presence of CdCl₂ is a key processing step for achieving high device performance. Although this treatment has been used over the past three decades [2–4], full understanding has not been achieved yet and this processing step requires careful research in some key areas. The defects signature in thin film CdTe has been identified as one of these key areas for careful investigation, in a recent comprehensive review [5], and this is the main subject of this publication.

This work presents photoluminescence (PL) studies carried out at 80 K on four different electroplated CdTe layers grown using three Cd-precursors. In this research programme, CdTe layers were electroplated using aqueous solutions of CdSO₄ [6], Cd(NO₃)₂ [7] and CdCl₂ [8] as the Cd-precursors, and TeO₂ solution as the Te-precursor. PL of these materials was studied to investigate the defects “finger prints”; thereby enabling the best performing Cd precursor to be selected for the electrodeposition of CdTe for photovoltaic applications. In the three cases described above, the CdTe was electroplated using a graphite anode; while in the fourth case, CdTe was grown using a platinum anode. The PL spectroscopy was used to examine the defects structure in the bandgap of the four nearly optimised CdTe thin films, and the results are compared with the PL

✉ I. M. Dharmadasa
Dharme@shu.ac.uk

¹ Materials and Engineering Research Institute, Sheffield Hallam University, Sheffield S1 1WB, UK

² Conn Centre for Renewable Energy Research, University of Louisville, Louisville, KY 40292, USA

spectra observed for two different bulk CdTe wafers purchased from industry.

2 Experimental

The CdTe layers used were electrodeposited on glass/FTO/CdS substrates using aqueous solutions containing Cd-precursor and TeO₂ solution. Two of the four different CdTe layers used in this work were grown using CdSO₄ precursor with two different anodes (Pt and graphite) [6]. The other two CdTe layers were grown using Cd(NO₃)₂ precursor [7] and CdCl₂ precursor [8] both with graphite anode as reported in recent publications. The chloride precursor was used in a 3-electrode system, with saturated calomel as the reference electrode, while the other precursors were used in 2-electrode systems. All Cd-precursors used were purchased from Fisher Scientific and the purity was 99 %. The solutions were electro-purified for ~100 h before deposition of CdTe layers. The concentration of the Cd-precursor in all cases was 1.0 M. pH value was at 2.00 ± 0.02 at the start of the growth and temperature was raised to 85 °C for the 2-electrode system, and to 70 °C for the 3-electrode system due to the temperature limit of the reference electrode. A dilute high purity (99.99 %) TeO₂ solution was added to the electrolyte at regular intervals in order to maintain a low level of Te in the bath. The four electroplated CdTe layers were grown by four different researchers using different chemicals and various growth parameters. Hence, these layers can be considered as different CdTe materials with the CdTe layer thickness in the range 1.0–2.0 μm. However, it should be noted that all four electroplated layers used in this work were grown at nearly optimised growth conditions established after a comprehensive research programme. The growth and full characterisation details are published in several PhD thesis [9–12] and a journal publication [6]. These nearly optimised materials also produce conversion efficiencies in the range 6–12 % [6, 11, 12], when used in fully fabricated glass/FTO/CdS/CdTe/Au devices. The main aim of this work is to examine the defect structure present within the bandgaps of these materials, and to decide which Cd-precursor produces the best CdTe layers for fabricating CdS/CdTe thin film solar cells. The second aim is to explore the effects on defect levels when heat treated in the presence of CdCl₂. The final aim is to explore the effects of electroplating CdTe using a CdCl₂ solution, and find out if the precursor will introduce a built-in CdCl₂ treatment during the growth.

In order to compare the finger prints of the defects existing in the thin film CdTe layers, together with that of melt-grown bulk CdTe, PL studies were also carried out on CdTe wafers purchased from industry (University Wafers Company in US). Dimensions of these wafers were

typically (10 × 10 × 1) mm³ and one surface was polished to a mirror finish with 0.5 μm size diamond paste. This paper also re-visits the PL results obtained in the past for CdTe wafers purchased from Eagle Pitcher in US, to compare with present results on thin film CdTe layers.

The PL work was carried out using a Renishaw inVia Raman Microscope with a 632 nm (~1.96 eV) He–Ne laser as the excitation source. Since the excitation source is in red, the light beam can easily penetrate through the thin films of 1.0–2.0 μm thick CdTe layers. Therefore, the PL results reported in this paper represent the changes within the bulk of the thin film. The surface area of ~25 μm² was excited by 14.8 mW laser beam. The detector used in this system is a combination of a diffraction grating and a CCD camera. The system is capable of measuring a wide range of energies. The samples were cooled to approximately 80 K using a Linkam THMS600/720 temperature controlled stage with liquid nitrogen and maintained at this temperature over the length of the PL measurements. The PL peaks in the energy range, 0.55–1.85 eV below the conduction band (CB) were explored in order to investigate any changes in the defect levels and the band-to-band electron transitions. Although there are other PL studies on CdTe [13–15] in narrow energy ranges due to limitations of the detectors used, this work examines a wide energy range from 0.55 to 1.85 eV to detect defect finger-prints.

After measuring the PL spectra of the as-deposited layers, CdCl₂ treatment was carried out in two steps. The first step was by treating the samples in ~1 % CdCl₂ aqueous solution and heat treating at 440 °C for 8 min. The second step was carried out by treating the samples again with ~1 % CdCl₂ aqueous solution and heat treating at 440 °C for 16 min. The aim here is to examine the trend in the changes of defect levels existing in the forbidden gap of CdTe during this processing step.

3 Results and discussion

The PL process can be understood by referring to the electron excitation and subsequent transitions taking place from the CB to defects and the valence band (VB), as shown in Fig. 1. When the CdTe surface is excited by laser light of 632 nm (1.96 eV), electrons are continuously pumped from VB to the CB. These electrons are then captured by electron traps (T_n), as they make the transition from the CB towards the VB, therefore emitting photons with different energies in order to create various PL peaks. Band-to-band electron transitions create a peak providing the energy bandgap of the material. In order to produce PL peaks, traps should be electron traps with high concentrations and large cross-sections, and the transitions must be radiative. In this PL set-up, only the electron trap levels,

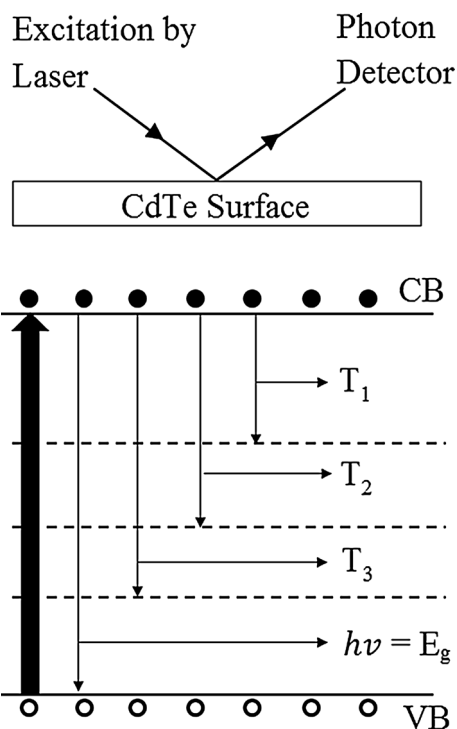


Fig. 1 Schematic diagram showing the excitation of electrons from the valence band to the conduction band and subsequent electron trapping due to defects in the bandgap as the electrons make transitions from the conduction band towards the valence band

~0.55 eV below the CB can be observed down to the VB edge due to the limitations of the detector system used.

3.1 Photoluminescence observations from thin films of CdTe

Typical PL spectra recorded at 80 K for the thin film CdTe layers (S1–S4) grown from different precursors are shown in Fig. 2. Five main PL peaks labelled T₁–T₄ and E_g can be

observed in the energy range, 0.55–1.85 eV as summarised in Table 1. The energy values corresponding to the maxima of these peaks are given in Table 1 together with their approximate energy spread. The peak positions at 80 K can be converted into room temperature values when necessary, using the rate of change of energy bandgap, (dE_g/dT) = -4.2 × 10⁻⁴ eV K⁻¹ as reported for CdTe [16]. The maxima of the peaks appear at 0.66, 0.79, 0.97, 1.37 and 1.50 eV at 80 K, indicating at least four deep defect bands situated in the explored energy range, below the CB minimum. The broad peak at 1.50 eV contains the energy bandgap of CdTe showing band-to-band electron transitions and labelled as “E_g” only for the purpose of discussion. This peak is broad due to various energy transitions on both sides of the energy gap of the material. The trap levels T₁, T₃ and T₄ are narrow, but the electron traps at 0.79 eV (T₂) spread over ±0.15 eV wide energy range. It is noteworthy that T₂ is a widely distributed defect and situated right in the middle of the bandgap. Therefore, these defects are very effective in recombination process, causing detrimental effects in PV performance. These defects kill photo-generated charge carriers through recombination and hence known as “killer centres” in II–VI semiconductors [17]. A good solar energy material should be free of these mid-gap killer centres.

It should be noted that the joining of two PL spectra in these measurements is taking place on the T₃ level. Therefore, the observation of a clear peak at T₃ is disturbed, but this feature can be observed in all PL spectra. However, the identification of a peak at 0.97 eV is not that difficult from these measurements on four different layers.

Although the defect level, T₄ also has a broader distribution, the probability of recombination of charge carriers through this level is very low due to its closeness to the VB. The E_g peak containing the band-to-band transition is also broad and extends beyond the bandgap of CdTe. The

Fig. 2 Typical photoluminescence spectra recorded at 80 K for four as-deposited CdTe layers using different Cd-precursors (Cd-sulphate, nitrate and chloride). The intensity of peaks are normalised to that of the band-gap emission peak, E_g

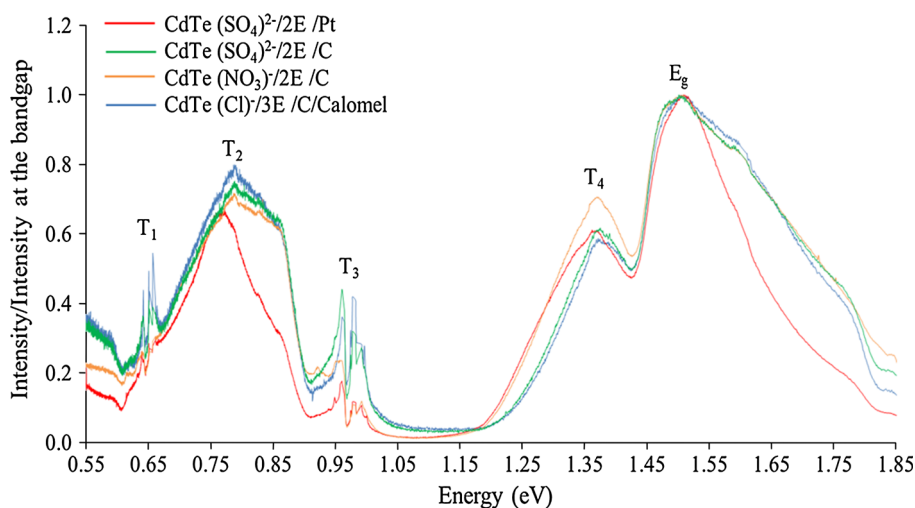


Table 1 Summary of electron trap levels (T_1 – T_4) and the energy bandgap peak (E_g) observed at 80 K for the four as-deposited CdTe layers

Sample ID	Material	$T_1 \pm 0.02$ (eV)	$T_2 \pm 0.15$ (eV)	$T_3 \pm 0.03$ (eV)	$T_4 \pm 0.08$ (eV)	E_g peak (eV)
S1	CdTe (SO_4^{2-})/2E/Pt	0.66	0.77	0.97	1.36	1.51
S2	CdTe (SO_4^{2-})/2E/C	0.66	0.79	0.97	1.37	1.50
S3	CdTe (NO_3^-)/2E/C	0.66	0.79	0.98	1.37	1.50
S4	CdTe (Cl^-)/3E/C	0.66	0.79	0.98	1.37	1.50

2E and 3E stands for 2-electrode and conventional 3-electrode systems respectively. Pt and C show the materials used for anodes

Growth conditions of the samples

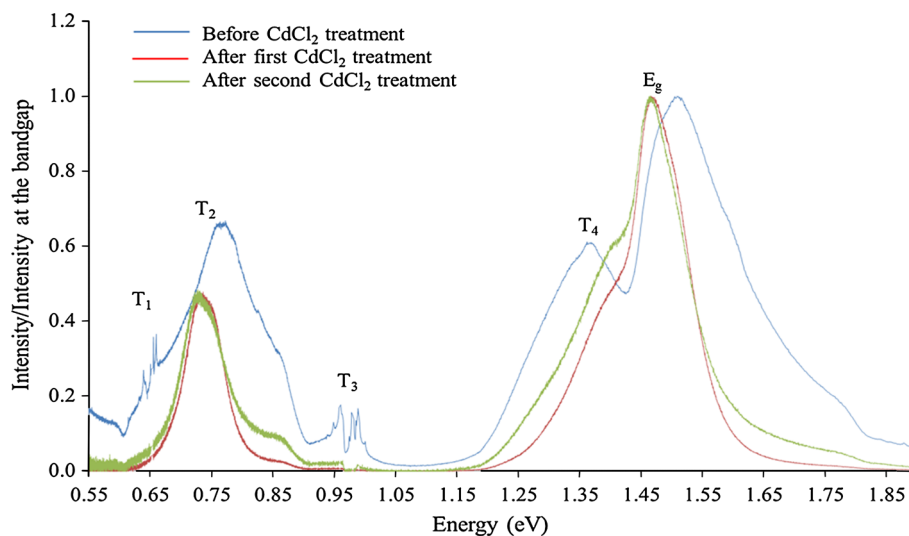
S1: 1.0 M CdSO_4 , low con. of TeO_2 , pH = 2.00, temp. = 85 °C, growth voltage = 2.238 V

S2: 1.0 M CdSO_4 , low con. of TeO_2 , pH = 2.00, temp. = 85 °C, growth voltage = 1.576 V

S3: 1.0 M CdNO_3 , low con. of TeO_2 , pH = 2.00, temp. = 85 °C, growth voltage = 1.253 V

S4: 1.0 M CdCl_2 , low con. of TeO_2 , pH = 2.00, temp. = 70 °C, growth voltage = 0.693 V

Fig. 3 Photoluminescence spectra for as-deposited, first CdCl_2 treated and second CdCl_2 -treated CdTe layers, electroplated using CdSO_4 precursor in 2-electrode system with Pt anode (S1)



emissions greater than E_g may arise due to the presence of S-rich $\text{CdS}_x\text{Te}_{(1-x)}$ alloy at CdS/CdTe interface, high temperature (80 K) PL measurements and high energy density excitations during the measurements. The emissions with energy greater than the bandgap could also occur due to quantum effects. The electroplated CdTe material consisting of grains in nano-scale could exhibit quantum effects in electron transitions creating photons with energy greater than the bandgap. The emissions with energy less than E_g can arise due to donor-to-acceptor type transitions, involving shallow energy levels, within the bandgap. It is also known that Te-rich $\text{CdS}_x\text{Te}_{(1-x)}$ alloy present on the CdTe side of CdS/CdTe interface has a low energy bandgap than that of CdTe due to “bandgap bowing effect” [18] and hence could broaden the peak on low energy side of the peak.

Figure 3 shows the PL spectra recorded for the CdTe layer (S1) electroplated using CdSO_4 precursor and 2-electrode system with Pt anode. The three spectra correspond to

Table 2 Summary of electron traps at 80 K for CdTe layers electroplated from CdSO_4 precursor using 2-electrode system with Pt anode (S1)

Energy (eV)	T_1	T_2	T_3	T_4	E_g
As deposited	0.66	0.77	0.97	1.36	1.51
CdCl_2 —step 1	–	0.73	–	1.39	1.47
CdCl_2 —step 2	–	0.73	–	1.39	1.47

the as-deposited and CdCl_2 treated CdTe in two steps. The observed peak details are summarised in Table 2, and a few major changes are clear from these results. The two defect levels at T_1 and T_3 completely disappear during CdCl_2 treatment. The broad distribution of T_2 narrows down and T_4 level reduces indicating drastic removal of defects from the bandgap. The broad peak E_g consists of several transitions, but sharpens after CdCl_2 treatment producing 1.47 eV for the bandgap of the material. This indicates the elimination of higher energy emissions due to coalescence of small

Fig. 4 Photoluminescence spectra for as-deposited, first CdCl₂ treated and second CdCl₂-treated CdTe layers electroplated using CdSO₄ precursor in 2-electrode system with graphite anode (S2)

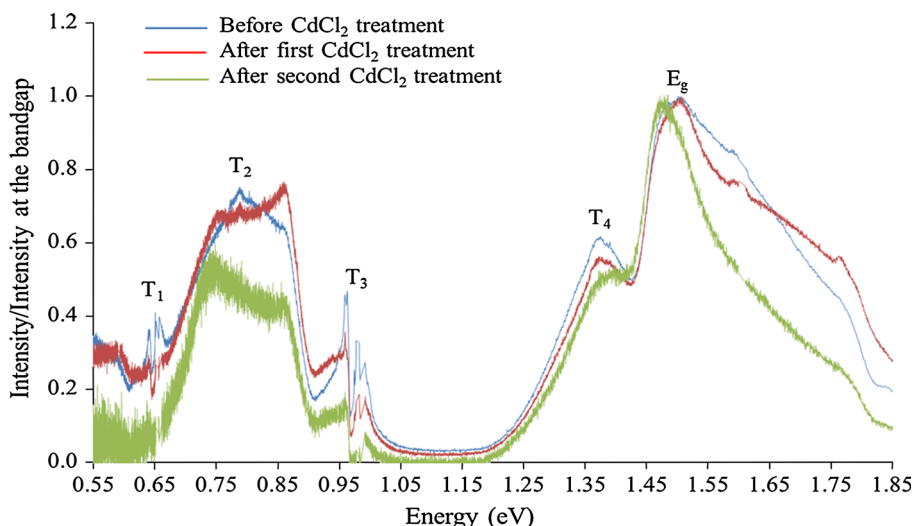


Table 3 Summary of electron traps at 80 K for CdTe layers electroplated from CdSO₄ precursor using 2-electrode system with graphite (C) anode (S2)

Energy (eV)	T ₁	T ₂	T ₃	T ₄	E _g
CdTe—As deposited	0.66	0.79	0.97	1.37	1.50
CdTe—CdCl ₂ —step 1	–	0.76	0.97	1.37	1.50
CdTe—CdCl ₂ —step 2	–	0.74	0.97	1.38	1.48

crystallites into large CdTe grains. This removes the quantum effects and therefore reduces larger values for E_g transitions.

Figure 4 and Table 3 show the PL spectra and details of defects for the CdTe layer (S2) grown from CdSO₄ precursor using 2-electrode system with graphite (C) anode. The same four defect levels were observed, and the disappearance of T₁ is clear after CdCl₂ treatment. Reduction of T₃ is evident but the defects are not completely removed. Although the intensities of T₂ and T₄ peaks have gone down, the distribution has not reduced. Clearly, the

layers are full of defects even after CdCl₂ treatment and these will have detrimental effects on device performance. It should be noted that each of the four layers under study was electroplated by a different researcher introducing various differences. At the same time, these layers are not yet fully optimised to achieve highest possible efficiency for solar cells.

Figure 5 and Table 4 present the PL spectra and the peak details for CdTe layers (S3) grown with Cd(NO₃)₂ precursor, using a 2-electrode system with graphite anode. The most striking observation is that the peak positions are in general very similar for all the CdTe layers. After CdCl₂ treatment, T₁ completely disappears and, T₃ peak still remains in this case. Although the intensity of T₂ has reduced considerably, the distribution remains the same. Intensity of T₄ first reduces and then increases with addition of more CdCl₂ to the treatment. The band-to-band emission peak sharpens by reducing the width of the peak. The bandgap value gets closer to 1.48 eV after CdCl₂ treatment, reducing the high energy PL emissions.

Fig. 5 Photoluminescence spectra for as-deposited, first CdCl₂-treated and second CdCl₂-treated CdTe layers electroplated, using Cd(NO₃)₂ precursor in 2-electrode system with graphite anode (S3)

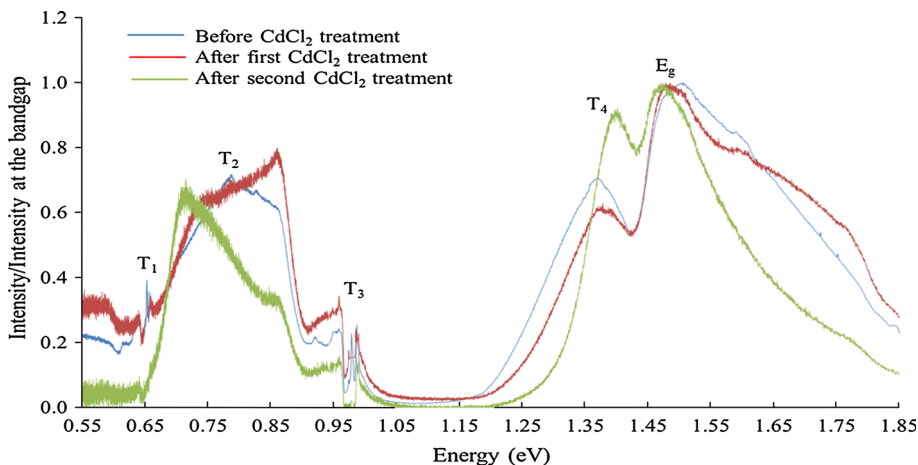


Table 4 Details of PL peaks at 80 K for CdTe layers electroplated using Cd(NO₃)₂ precursor and 2-electrode system with graphite anode (S3)

Energy (eV)	T ₁	T ₂	T ₃	T ₄	E _g
CdTe—As deposited	0.66	0.79	0.98	1.37	1.50
CdTe—CdCl ₂ —step 1	0.66	0.86	0.99	1.38	1.48
CdTe—CdCl ₂ —step 2	–	0.71	0.99	1.40	1.48

Figure 6 and Table 5 show similar results for CdTe layers (S4) grown using CdCl₂ precursor, in a 3-electrode system with a graphite anode. A saturated calomel electrode was used as the reference electrode in this system since Hg is not detrimental to CdTe based solar cells [19]. These layers provide well-defined PL spectra with the most accurate peak positions. All five peaks in the as-deposited layer are identical in energy position terms to those of CdTe grown from other precursors, but show drastic changes after CdCl₂ treatment. The T₁ and T₃ defect levels are completely annealed-out during the CdCl₂ treatment. Considerable reduction of the energy distribution of T₂ from ~0.34 to ~0.09 eV is extremely interesting to note. Drastic reduction of the intensity of T₄ and sharpening of the bandgap peak are excellent results to observe. In particular, the drastic reduction of mid-gap “killer centres” at T₂ is good news for photovoltaic devices. It should be noted that the main difference in this layer is the electroplating from CdCl₂ precursor. Therefore the built-in CdCl₂ treatment is already there, even during the materials growth by depositing molecule by molecule. Therefore the effect of CdCl₂ treatment should be highest in this material. Changes at the band-to-band transitions are drastic and noteworthy. Formation of highly crystalline CdTe with low defects, in the presence of Cl[−] is clear from these results. It seems that Cl[−] ions are acting as a fluxing agent for the growth of CdTe with large crystals and low defect density. Nano-scale crystals coalesce to form a few micron size

Table 5 Details of PL peaks at 80 K for CdTe layers (S4) electroplated using CdCl₂ precursor and 3-electrode system with graphite anode and saturated calomel reference electrode

Energy (eV)	T ₁	T ₂	T ₃	T ₄	E _g
As deposited	0.66	0.79	0.98	1.37	1.50
CdCl ₂ —step 1	–	0.76	–	1.39	1.51
CdCl ₂ —step 2	–	0.76	–	1.39	1.51

grains after CdCl₂ treatment. This has clearly shown by SEM work [10–12, 20] but not presented in this paper since this is out of context.

A summary of PL studies on all four CdTe layers are given in Table 6. Trap levels for both as-deposited and CdCl₂ treated (after second stage) samples are shown for comparison. Four trap levels have been observed for all CdTe layers in the explored energy range. T₂ situated at the mid-gap is a broad peak spreading over ~0.30 eV range, and will be more effective in recombination of photo-generated charge carriers created during PV action under illumination. This broad peak could consist of numerous PL peaks, but it is not possible to separate these due to close distributions of un-known defects. Therefore quantitative descriptions through curve-fitting are not accurate and possible, and our descriptions are limited only to qualitative explanations in all cases.

When heat treated in the presence of CdCl₂, T₁ and T₃ completely reduce in some samples, while others show a considerable reduction. T₂ is the main defects band present right in the middle of the bandgap and distributed in a wide energy range of ~0.30 eV. In other words, this broad peak could include a large number of PL peaks arising from closely situated defect levels forming a broad PL band. These are the most detrimental defects for PV action, with the highest probability of recombination process. T₄ appears at (1.36–1.40) eV, with varying intensity after CdCl₂ treatment. Therefore, as graphically shown in Fig. 7, CdCl₂

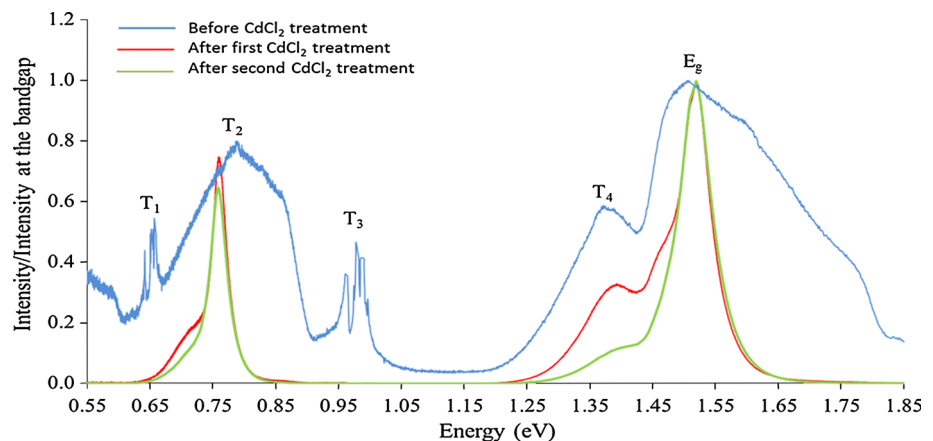
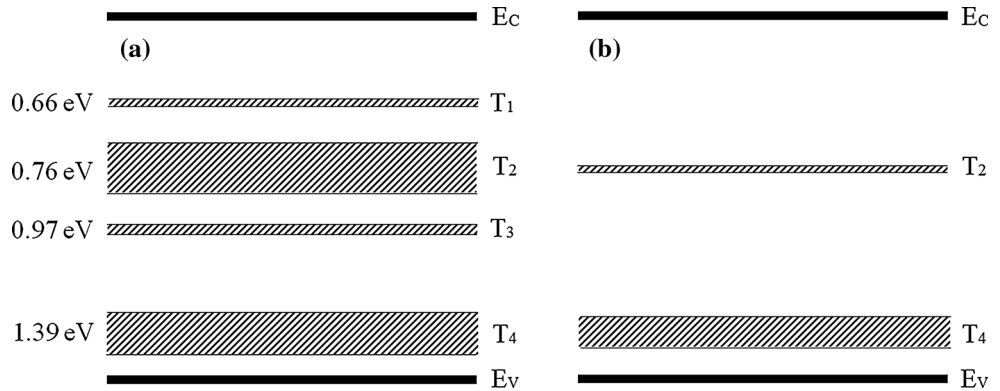
Fig. 6 Photoluminescence spectra for as-deposited, first CdCl₂-treated and second CdCl₂-treated CdTe layers (S4) electroplated using CdCl₂ precursor and 3-electrode system with graphite anode and saturated calomel reference electrode

Table 6 Summary of observed PL peaks at 80 K for four different CdTe layers electroplated from three different Cd-precursors (Cd-sulphate, nitrate and chloride)

Growth details	Material condition	T ₁ (eV)	T ₂ (eV)	T ₃ (eV)	T ₄ (eV)	E _g (eV)
S1—CdTe-(SO ₄ ²⁻)/2E/Pt	As-deposited	0.66	0.77	0.97	1.36	1.51
	CdCl ₂ treated	–	0.73	–	1.39	1.47
S2—CdTe-(SO ₄ ²⁻)/2E/C	As-deposited	0.66	0.79	0.97	1.37	1.50
	CdCl ₂ treated	–	0.74	0.97	1.38	1.48
S3—CdTe-(NO ₃ ⁻)/2E/C	As-deposited	0.66	0.79	0.98	1.37	1.50
	CdCl ₂ treated	–	0.71	0.99	1.40	1.48
S4—CdTe-(Cl ⁻)/3E/C	As-deposited	0.66	0.79	0.98	1.37	1.50
	CdCl ₂ treated	–	0.76	–	1.39	1.51

Fig. 7 A graphical summary of defects finger-print observed at 80 K for, **a** as-deposited and, **b** CdCl₂ treated thin films of CdTe grown by electroplating



treatment removes radiative defects clearing the bandgap of CdTe. The spread of the defect bands have been obtained using the width of PL peaks to represent distribution of defects within the energy band gap.

The most striking result is that the four defect levels observed for thin film CdTe are very similar to those observed for bulk CdTe wafers. The defect level positions in bulk CdTe have been observed by many techniques such as Schottky barrier measurements, Deep Level Transient Spectroscopy, Ballistic Electron Emission Microscopy and PL [17, 21, 22]. Three defect levels reported for bulk CdTe; 0.65, 0.73 and 0.96 eV below the CB are exactly coincide with T₁, T₂ and T₃ levels observed for thin films of CdTe. The T₄ seems to be introduced and enhanced by CdCl₂ heat treatment.

After CdCl₂ treatment, the bandgap of CdTe layer is in the range (1.47–1.51) eV. This bandgap value at 80 K corresponds to (1.36–1.42) eV at room temperature, which agrees well with the bandgap of bulk CdTe [17].

3.2 Photoluminescence observations from bulk CdTe material

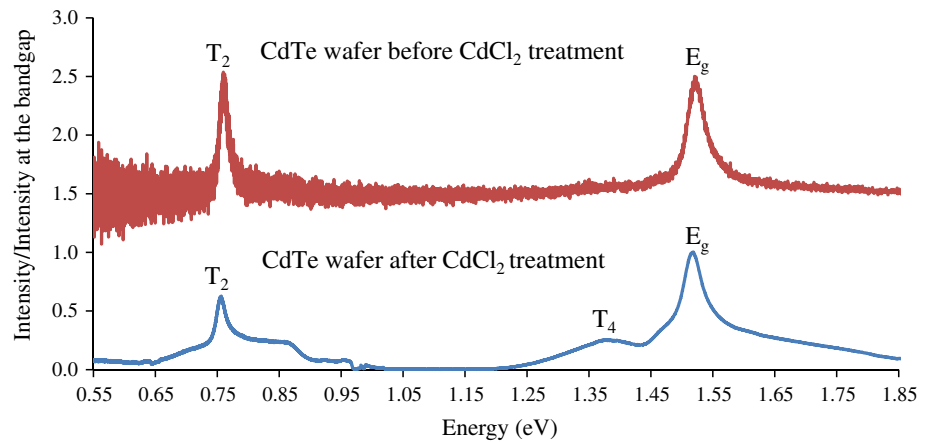
3.2.1 Bulk CdTe from University Wafers Company

In order to compare the PL results of thin films of CdTe with bulk material, (10 × 10 × 1) mm³ wafers were purchased from University Wafers Company in the United

States and the PL measurements were carried out under similar conditions, on polished surfaces. In order to observe any useful changes on the surface, these wafers were also treated with CdCl₂ and heat treated at 440 °C for 20 min. The surface was then rinsed well with de-ionised water and the PL spectra were recorded at 80 K in the same measurement system.

Figure 8 shows the PL spectra recorded for polished CdTe wafer before and after CdCl₂ treatment. As-received material shows two sharp peaks corresponding to 0.76 eV (T₂) mid-gap defects and 1.52 eV (E_g) energy gap peak of the material. These are identical to the two peaks, T₂ and E_g observed for thin films of CdTe. After CdCl₂ treatment, T₂ level shows slight broadening and additional peak at 1.39 eV (T₄) appears, showing that these changes are induced by CdCl₂ treatment on the surface layer. A review [23] by Fernández on PL and cathodoluminescence (CL) also summarize the increase of this particular level upon CdCl₂ treatment. Hernández-Fenollosa et al. [15] shows from their PL studies, that the 1.36 eV level rapidly increase during HCl treatment in the presence of oxygen. This information is extremely important in understanding what happens during this key processing step. The conclusion is that this additional defect level, T₄ emerges due to Cd-richness or the incorporation of Cl in CdTe in the presence of oxygen. This PL observation is also very similar to CL work reported by Mazzamuto et al. [24]. These authors reported the development of this peak at

Fig. 8 Photoluminescence spectra recorded before and after CdCl_2 treatment, for bulk CdTe wafers purchased from University Wafers Company. These wafers were produced using a melt-growth technique and the dimensions of the wafers used were $(10 \times 10 \times 1) \text{ mm}^3$



1.39 eV when Freon (CHFCl_2) gas pressure in the heating chamber is gradually increased during the heat treatment of close space sublimation (CSS) grown CdTe thin films. Since there are no additional Cd involved in this treatment, Cd-richness can be ruled out with confidence. This provides us a firm conclusion of the origin of this defect at 1.39 eV (T_4), below the CB edge. Cl interacts with CdTe lattice forming a defect level at 1.39 eV, very close to the VB. This level therefore, can act as a shallow acceptor in CdTe increasing the acceptor concentration (N_A) within the material. This information is helpful in understanding Cl as an amphoteric dopant. At ppm level, when Cl displaces Te atoms in the lattice, it is a well-known donor in CdTe [17]. However, when Cl concentration is high as in the case of CdCl_2 treatment, and interacts with CdTe layer, it produces an acceptor like defect at 1.39 eV (T_4), acting as a p-type dopant in CdTe. The presence of oxygen seems to catalyse this interaction [15]. The nature of interaction of Cl^- within CdTe layer is not-known at present, and extra information is needed to draw firm conclusions. The final electrical conductivity type depends on the resultant value of ($N_D - N_A$) in the material. This value can also depend on heat treatment temperature and the duration.

It is really striking to see the similarity in the PL spectra of commercially available CdTe bulk materials and that of electroplated CdTe thin films grown using CdCl_2 precursor (S4), after CdCl_2 treatment. These two spectra are plotted in Fig. 9 for direct comparison. It is clear that the thin film CdTe layers with thickness of the order of $1.0 \mu\text{m}$ can be grown with comparable defect levels in the bulk CdTe bandgap.

3.2.2 Bulk CdTe from Eagle Pitcher

It is also worth re-visiting the PL measurements carried out on bulk CdTe wafers purchased from Eagle Pitcher, in the past by the main author [25]. Figure 10 shows the PL spectra obtained at 4 K, together with corresponding X-ray photoelectron spectra (XPS) of the surfaces investigated. The

CdTe surfaces were mechanically polished and chemically etched to produce Te-rich or Cd-rich surface layers, and the PL spectra were recorded under same experimental conditions. The Te-richness and Cd-richness were confirmed using XPS experiments carried out on these surfaces [26].

Figure 10 shows the defect levels observed by purposely modifying the CdTe surfaces by chemical etching. The energy values can be converted to 80 K for comparison using the rate of change of the bandgap given in Sect. 3.1. The main defect levels observed at 80 K for bulk materials and the CdTe thin films grown using CdCl_2 precursor are summarised in Table 7. The results presented in this paper show that defects present in CdTe are common for at least six different CdTe materials produced with different conditions. The heat treatment in the presence of CdCl_2 turns the material into electronic grade layers with only two or three deep defect levels present in them. The most important results observed from Fig. 10 are that, T_2 is dominant for Te-rich layers and T_3 and T_4 are dominant for Cd-rich CdTe layers. This provides us with a method to control deep levels in CdTe material surfaces.

In addition to the PL results summarised in Table 7 for six different CdTe layers studied in this work, it is interesting to compare with the PL work carried out on CSS-grown CdTe layers, which produce highest efficiencies at present for CdS/CdTe solar cells. Ferekides et al. [13] have carried out PL on CSS-CdTe in the near bandgap region (1.24–1.65 eV) in 2000. They observed the two PL bands at 1.52 and 1.36 eV, and reported the emergence of 1.36 eV level after CdCl_2 treatment. Hernández-Fenollosa et al. [15] carried out PL work on CSS-CdTe grown at ANTEK, in the energy range 1.20–2.50 eV to study defect levels related to both CdTe and CdS. This work also detected the two PL bands at 1.52 and 1.36 eV related to CdTe. The six CdTe layers studied in this work and the PL on CSS-CdTe clearly show that 1.52 eV is related to the band-to-band emissions and 1.36 eV band is the one related to chloride treatment and hence responsible for improved device performance.

Fig. 9 Photoluminescence spectra of bulk CdTe wafers and electroplated CdTe thin films from chlorides (S4), after CdCl₂ heat treatment. Note the cleaner bandgap in the CdCl₂ treated CdTe thin film grown using CdCl₂ precursor, with a built-in CdCl₂ treatment

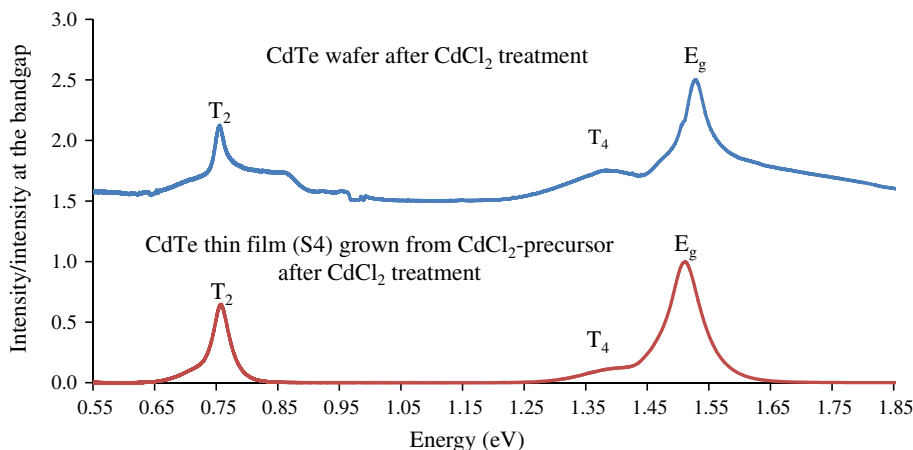


Fig. 10 The XPS spectra [26] of Te-rich and Cd-rich CdTe surfaces and their corresponding PL spectra obtained at 4 K [25]. The CdTe wafers were purchased from Eagle Pitcher in United States. The spectra (a–c) corresponds to PL from Te-rich surfaces and (d–f) correspond to PL from Cd-rich surfaces. Note the observation of four peaks, T₂, T₃, T₄ and E_g with very similar energies observed for thin films of CdTe

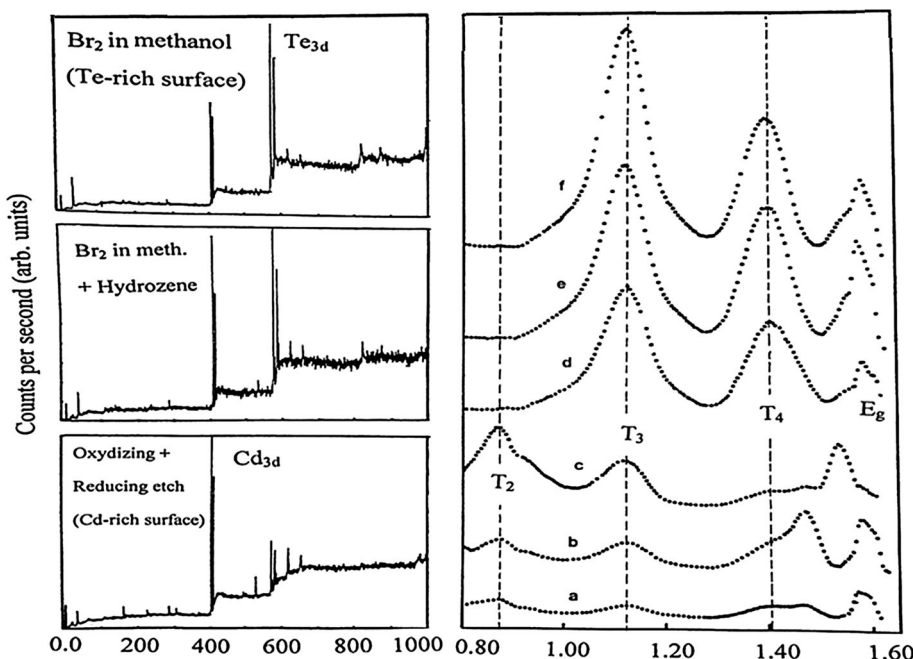


Table 7 Summary of defect levels observed from PL, for bulk CdTe from University Wafers Company, and Eagle Pitcher, and for thin film CdTe layers grown using CdCl₂ precursor (S4) and after CdCl₂ treatment

Material	T ₂ (eV)	T ₃ (eV)	T ₄ (eV)	E _g (eV)
Bulk CdTe (University Wafers Company)	0.76		1.39	1.52
Bulk CdTe (Eagle Pitcher)	0.84	1.09	1.37	1.52
Thin films of CdTe grown with CdCl ₂ precursor after CdCl ₂ treatment (S4)	0.76		1.39	1.51

4 Implications of deep defect levels on CdTe based solar cells

4.1 Effects on materials

It is now worth looking at the summary of PL results observed for both thin films and bulk CdTe materials. It is

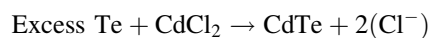
evident that there are at least four main discrete defect levels existing in the bandgap of CdTe. It is a striking result to observe deep level defects at very similar energy values (see Tables 6, 7) for four different thin films grown differently using various Cd-precursors and for two different bulk CdTe materials grown at two commercial companies. In addition T₄ and E_g peaks are identical for CSS grown

CdTe also. It is also noteworthy that T_1 , T_2 and T_3 levels observed for CdTe thin films are identical to three levels 0.65, 0.73 and 0.96 eV observed for bulk CdTe material [17, 21, 22]. This means that these defects must be arising from native defects in CdTe.

The observations in Fig. 10 for chemically etched bulk CdTe surfaces show that the intensities of defect-related peaks are much higher than those of the bandgap peak. This means that the electron transitions from E_c to defects are much stronger than those from E_c to the E_v . In opto-electronic device applications, these types of transitions are not very useful. However, the peak intensities shown in Fig. 6 and Table 8 for CdTe thin films grown using CdCl_2 precursor show that the E_g peak is much higher than the defect related peaks. This is the feature necessary for solar energy materials to fabricate efficient solar cells. A material with low intensity defect peaks will produce better devices. The counts of E_g peak for as-deposited material has increased from 8143 to 514,331 after the second CdCl_2 treatment. This clearly shows that defects in the bandgap have been drastically annealed-out and the band-to-band transitions have increased. This is the main reason that the CdCl_2 treatment is essential in order to fabricate efficient CdTe solar cells.

The PL observations in Fig. 10 also help in drawing another important conclusion. In Te-rich surfaces, defects (T_2) in the mid-bandgap are dominant, and in Cd-rich surfaces, defects in lower half of the bandgap (T_3 and T_4) are dominant. This observation is also confirmed by the CdCl_2 treatment of thin film CdTe layers presented in this paper. Results summarised in Table 6 and Fig. 7 clearly show that CdCl_2 treatment removes the trap levels at T_1 and T_3 , and drastically reduce the wide distribution of T_2 to a narrow distribution level. These are the defect levels situated towards the middle of the bandgap and related to the Te-richness of CdTe materials. Out of the two elements, Cd and Te in CdTe, Te is the easiest element to discharge first and deposit during electroplating (E° for Te is +0.593 V, and E° for Cd is -0.403 V with respect to hydrogen reference electrode). Therefore Te can be precipitated [27–29] within the layer or form a thin layer of Cd_xTeO_y on the surface [30]. Hence, most of the as-deposited CdTe layers have Te-rich nature and therefore T_1 and T_2 trap levels are dominant. However, when these layers are heat treated in the presence of CdCl_2 on the surface, excess Te converts

into useful CdTe phase improving the composition towards stoichiometric CdTe layers [5].



The presence of Cl^- in this process also helps in recrystallisation and doping of the CdTe. In fact, the CdCl_2 treatment converts Te-richness of the initial CdTe layer into Cd-richness, and also reduces defects at T_1 and T_2 . This produces a CdTe layer with fairly clean bandgap removing defects in the mid-gap (see Fig. 7). The same process increases the band-to-band transitions of electrons, as a result of removal of mid-gap defect levels (see Table 8) producing a better solar energy material.

The results presented in this paper also helps in deciding which precursor is more suited to electrodeposit high quality CdTe layers. In the past, almost all electroplating of CdTe were carried out using CdSO_4 precursor [31–33] and $\text{Cd}(\text{NO}_3)_2$ or CdCl_2 were not properly explored. The work presented in this paper strongly indicate the CdTe layers grown from CdCl_2 have much cleaner band gaps (see Fig. 6), and hence should produce improved devices. Detailed work is in progress to select best precursor for CdTe electroplating and fabrication of high efficiency devices [6–9].

4.2 Effects on devices

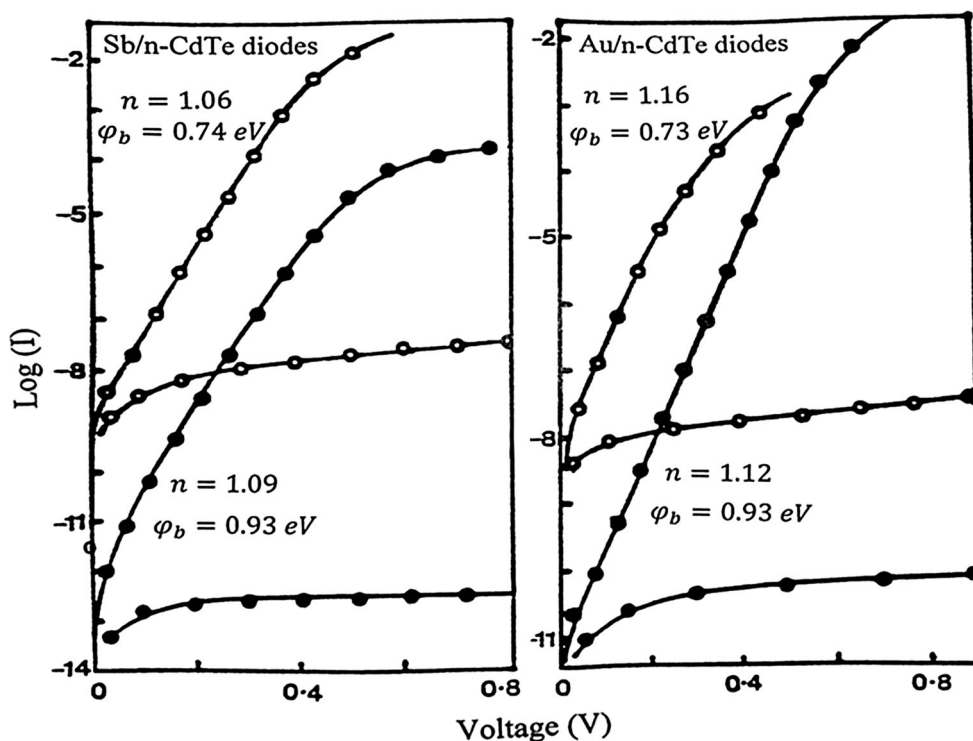
At this point, re-visiting the electrical contacts to II–VI compounds and published work in the past [21, 26, 34, 35], showing preparation of Cd-rich and Te-rich CdTe surfaces leading to the formation of different Schottky barriers at metal/n-CdTe interfaces is highly relevant. Figure 11 shows I–V characteristics of Schottky diodes produced by metal/n-CdTe interfaces. The barrier heights are independent of the metal used, and the same metal (Sb, Au, etc.) produces low barriers (~ 0.72 eV) on Te-rich surfaces and high barriers (~ 0.96 eV) on Cd-rich surfaces. In these cases, the Fermi level pins at T_2 for Te-rich surfaces and at T_3 for Cd-rich CdTe surfaces. It is obvious that once the defects at T_1 , T_2 and T_3 are removed from the bandgap, extremely large Schottky barriers can be produced by pinning the FL at T_4 (~ 1.24 eV at room temperature). This is indeed routinely observed in our CdTe devices made out of electrodeposited Cd-rich CdTe layers.

The most striking effect is the observation of similar discrete barriers for thin film CdTe layers [34]. From the results presented in this paper, it is clear that the defect levels in CdTe are common at least for six different CdTe materials and play a very important role in Schottky barrier formation at metal/n-CdTe interface. This Fermi level pinning strongly affects the performance of CdTe based solar cells as published before [21, 26, 34, 35]. Pinning the Fermi level at the defect level at T_3 (~ 0.92 eV room temperature)

Table 8 Intensity of band-to-band electron transitions (E_g peak) for CdTe thin films grown using CdCl_2 precursor (S4), and after CdCl_2 treatment

S4—CdTe (Cl^-) ^{3E/C}	E_g peak intensity (photon counts)
As-deposited	8143
CdCl_2 treated—step 1	60,740
CdCl_2 treated—step 2	514,331

Fig. 11 Typical Schottky diode characteristics produced on Te-rich and Cd-rich CdTe wafers (Eagle Pitcher) with Sb and Au electrical contacts. Barrier heights are independent of the metal used and are created due to strong Fermi level pinning positions at T_2 level for Te-rich and at T_3 level for Cd-rich CdTe [21, 26, 34, 35]



or at T_4 (~ 1.24 eV at room temperature) produces high potential barriers at metal/n-CdTe interfaces creating excellent rectification properties exceeding $\sim 10^8$ rectification factors at 1.0 V. The presence of T_4 level at ~ 1.36 eV at low temperature for CSS-CdTe is noteworthy and this level corresponds to ~ 1.24 eV at room temperature.

The most recent ultra-violet photoemission spectroscopy work [36] on electroplated CdTe thin films confirmed that the Fermi level settles in the upper-half of the bandgap after $CdCl_2$ treatment. This means that under $CdCl_2$ treatment, N_D remains greater than N_A and hence the material remains n-type after $CdCl_2$ treatment. It is also extremely important to note Schulmeyer et al. [37] work on CSS-CdTe layers obtained from ANTEK. These authors performed XPS studies on $CdCl_2$ treated CSS-CdTe layers and determined the position of the Fermi level in CdTe, and measured the efficiency of fully fabricated CdS/CdTe device structures. They reported that the highest efficiencies are observed when the Fermi level is ~ 0.85 eV above the VB. This means that the Fermi level has settled ~ 0.60 eV below the CB minimum, and material remained n-type after $CdCl_2$ treatment. Their work also confirms the production of highest efficiency values when devices are fabricated with CSS grown n-type CdTe layers.

In order to make high performing solar cells, one needs to grow high quality n-type CdTe layers without defects at T_1 , T_2 and T_3 . The material should have high concentrations of T_4 defects influenced by $CdCl_2$ treatment, in order to pin the Fermi level at the vicinity of T_4 level (~ 1.24 eV

at room temperature). Combining all the results presented in this paper and the most useful and relevant information published in the literature, the energy band diagram of the most efficient CdS/CdTe solar cell is shown in Fig. 12. As at present, the mid-gap T_2 defect related to Te-richness is still present in the CdTe bandgap. Complete removal of T_1 , T_2 and T_3 and pinning of the Fermi level at the T_4 defect level will produce high performing devices reducing recombination process. This Fermi level pinning can be enhanced by adding p-dopants such as Cu, Sb, As, Bi, etc. to the electrical contact material. Also by adding p-type and wide bandgap semiconducting layers such as p-ZnTe and p-type organic polymers on CdTe, the Fermi level can be forced to keep very close to the VB of CdTe. The barrier height, Φ_b at the back contact can be further improved using MIS-type electrical contacts forming barrier heights exceeding the energy gap of CdTe. This will lead to production of large V_{oc} values for this solar cell. This device architecture as proposed in 2002 [34] and afterwards [35], is a tandem device of an n-n hetero-junction in the front connected in parallel to a large Schottky barrier at the back. In this parallel connection, CB is connected to CB, instead of connecting the CB to the VB in series connection or conventional tunnel-junction approach [38, 39]. In this device structure with parallel connection of the two junctions, V_{oc} remains constant and the current density (J_{sc}) adds up from two devices. MIS type electrical contacts could produce barrier heights greater than the bandgap of CdTe when optimised and hence produce high V_{oc} values.

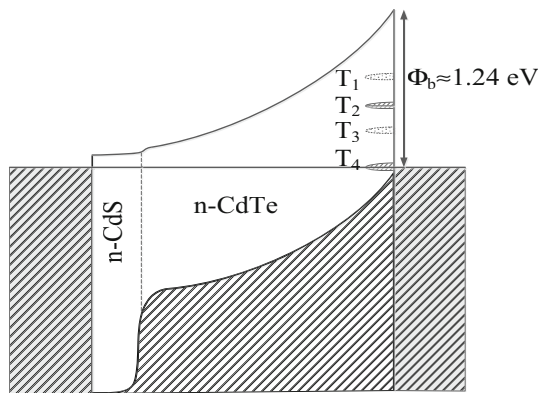


Fig. 12 Energy band diagram of CdS/CdTe solar cell depicting four main deep levels observed using PL studies carried out in this work. The Fermi level is pinned at T_4 level

Since CdTe can easily be produced either in p-type or n-type electrical conduction, there exists two types of device structures; genuine single p–n junctions, and combined two junctions as shown in Fig. 12. Highest efficiencies are produced by the devices fabricated with n-CdTe [37], but all interpretations in the past were given in terms of a simple p–n junction. This has created a severe confusion in the CdS/CdTe development field and hence the conversion efficiency stagnated at $\sim 16\%$ [40, 41] for over two decades. Proper understanding of the materials and device issues, designing and developing the appropriate device architectures, optimising the materials growth and device processing steps will lead to producing high performing CdS/CdTe solar cells with efficiencies well above the current values of 21.5% in the near future.

5 Conclusions

The PL results presented in this paper and other highly relevant information from the literature lead to drawing the following important conclusions.

- All four CdTe layers electroplated using sulphate, nitrate and chloride of cadmium, pre-cursors exhibit four electron traps (T_1 , T_2 , T_3 and T_4) situated at similar energy positions. The bulk CdTe wafers purchased from Eagle Pitcher and etched surfaces also exhibit three defects at T_2 , T_3 and T_4 . Materials from University Wafers Company show only one defect level at T_2 in the mid-gap.
- When PL intensities of the electroplated materials are compared with those of the chemically etched bulk material surface, band-to-band transitions are strong in thin film CdTe layers. This indicates the low-trap concentrations in electroplated materials after CdCl_2 treatment.

- After CdCl_2 treatment, T_1 , T_2 and T_3 are completely annealed-out or show considerable reduction in concentration. This reduction is a positive effect for device performance.
- CdCl_2 treatment drastically reduces the mid-gap killer centres situated at T_2 level. Wide defects distribution (~ 0.30 eV) reduces to a narrow defect band (~ 0.09 eV) and the intensity also reduces by considerable amounts. This will have a drastic and positive effect on improvement of solar cell performance by reducing recombination of photo-generated charge carriers.
- The two defect levels T_1 and T_2 , situated in the mid-gap are closely related to Te-richness in CdTe layers. CdCl_2 treatment converts the Te-richness towards Cd-richness, reducing precipitated Te, and drastically removing mid-gap defects.
- Out of all four CdTe layers studied in this work, the material grown using CdCl_2 precursor seems to produce a better material with a cleaner bandgap. This material is comparable to University Wafers Company—CdTe in terms of defect levels. The built-in CdCl_2 treatment during the growth of the layer may be the most possible reason. However, it should be noted that all these layers are grown by four different researchers and are grown at nearly optimised conditions.
- All six CdTe layers studied in this work, and reported results for CSS-CdTe have the defect level at T_4 , enhanced by CdCl_2 treatment. Fermi level pinning at T_3 (~ 0.92 eV at room temperature) or at T_4 (~ 1.24 eV at room temperature) produces large Schottky barriers at n-CdTe/metal interface and hence produces high performing CdS/CdTe solar cells. The most desirable level to pin the Fermi level is ~ 1.24 eV below the CB.

Acknowledgments Authors would like to thank and acknowledge the contributions made by Paul Bingham, Mohammed Madugu, Olajide Olusola and Ayotunde Ojo, through technical discussions.

Conflict of interest The authors declare that they have no conflict of interest.

References

- First Solar pushes verified CdTe cell efficiency to record 21.5% , http://www.pv-tech.org/news/first_solar_pushes_verified_cdte_cell_efficiency_to_record_21.5. Press Release on 5 Feb 2015
- N. Nakayama, H. Matsumoto, K. Yamaguchi, S. Ikagami, Y. Hioki, Ceramic thin film CdTe solar cell. *Jpn. J. Appl. Phys.* **15**, 2281–2282 (1976)
- A. Abbas, G.D. West, J.W. Bowers, P. Isherwood, P.M. Kaminski, B. Maniscalco, P. Rowley, J.M. Walls, K. Barricklow,

- W.S. Sampath, K.L. Barth, The effect of cadmium chloride treatment on close-spaced sublimated cadmium telluride thin-film solar cells. *IEEE J. Photovolt.* **3**(4), 1361–1366 (2013)
4. X. Huo, X. Peng, W. Liu, X. Mo, G. Chen, S. Wang, J. Chu, Comparison between the effects of CdCl₂ heat treatment on CdTe films prepared by RF magnetron sputtering and close spaced sublimation methods. *J. Mater. Sci. Mater. Electron.* (2013). doi:10.1007/s10854-013-1121-6
 5. I.M. Dharmadasa, Review of the CdCl₂ treatment used in CdS/CdTe thin film solar cell development and new evidence towards improved understanding. *Coatings* **4**(2), 282–307 (2014). doi:10.3390/coatings4020282
 6. O.K. Echendu, F. Fauzi, A.R. Weerasinghe, I.M. Dharmadasa, High short-circuit current density CdTe solar cells using all-electrodeposited semiconductors. *Thin Solid Films* **556**, 529–534 (2014). doi:10.1016/j.tsf.2014.01.071
 7. H.I. Salim, V. Patel, A. Abbas, M. Walls, I.M. Dharmadasa, Electrodeposition of CdTe thin films solar cells using nitrate precursor. *J. Mater. Sci. Mater. Electron.* **26**(5), 3119–3128 (2015)
 8. N.A. Abdul-Manaf, H.I. Salim, M. Madugu, I.M. Dharmadasa, Electrodeposition of CdTe thin films using chloride precursor for the application in solar cells, PVSAT-11 (University of Leeds, UK, 2015)
 9. D.G. Diso, Research and development of CdTe based thin film solar cells, PhD thesis, Sheffield Hallam University, 2011
 10. A.R.A. Weerasinghe, Solar cells based on electrodeposited thin films of ZnS, CdS, CdSSe and CdTe, PhD thesis, Sheffield Hallam University, 2013
 11. O.K. Echendu, Thin film solar cells using all-electrodeposited ZnS, CdS and CdTe materials, PhD thesis, Sheffield Hallam University, 2014
 12. F. Fijay, Research and development of CdS/CdTe solar cells incorporating ZnTe layers, PhD thesis, Sheffield Hallam University, 2015
 13. C.S. Ferekides, D. Marinik, V. Viswanathan, B. Tetali, V. Palekis, P. Selvaraj, D.L. Morel, *Thin Solid Films* **361–362**, 520–526 (2000)
 14. K.J. Price, D. Greuca, D. Shvydka, A.D. Compaan, Photoluminescence of CdTe:Cu and CdS:Cu. (The University of Toledo, Toledo, 2000), p. 43606
 15. M.A. Hernández-Fenollosa, D.P. Halliday, K. Durose, M.D. Campo, J. Beier, Photoluminescence studies of CdS/CdTe solar cells treated with oxygen. *Thin Solid Films* **431–432**, 176–180 (2003)
 16. Y.F. Tsay, S.S. Mitra, J.F. Vetelino, *J. Phys. Chem. Solids* **34**, 2167 (1973)
 17. K. Zanio, *Semiconductors and Semimetals, volume 13, Cadmium Telluride* (Academic Press, New York, 1978)
 18. D.A. Wood, K.D. Rogers, D.W. Lane, J.A. Coath, Optical and electrical characterisation of Cd_xTe_(1-x) thin films for solar cell applications. *J. Phys. Condense. Matter* **12**, 4433–4450 (2000)
 19. I.M. Dharmadasa et al., Un-published experimental results
 20. I.M. Dharmadasa, P.A. Bingham, O.K. Echendu, H.I. Salim, T. Druffel, R. Dharmadasa, G.U. Sumanasekera, R.R. Dharmasena, M.B. Dergacheva, K.A. Mit, K.A. Urazov, L. Bowen, M. Walls, A. Abbaas, Fabrication of CdS/CdTe-based thin film solar cells using an electro-chemical technique. *Coatings* **4**, 380–415 (2014). doi:10.3390/coatings4030380
 21. I.M. Dharmadasa, Recent developments and progress on electrical contacts to CdTe, CdS and ZnSe with special reference to barrier contacts to CdTe. Invited review paper. *Prog. Cryst. Growth Charact.* **36**(4), 249–290 (1998)
 22. T.L. Chu, in *Chapter 3 of “Current Topics in Photovoltaics”*, vol. 3, ed. by T.J. Coult, J.D. Meakin (Academic Press, New York, 1988), p. 242
 23. P. Fernández, Defect structure and luminescence properties of CdTe based compounds. *J. Optoelectron. Adv. Mater.* **5**(2), 369–388 (2003)
 24. S. Mazzamuto, L. Vailant, A. Bosio, N. Romeo, N. Armani, G. Salvati, A study of the CdTe treatment with a Freon gas such as CHF₂Cl. *Thin Solid Films* **16**, 7079–7083 (2008)
 25. Z. Sobiesierski, I.M. Dharmadasa, R.H. Williams, Correlation of photoluminescence measurements with the composition and electronic properties of chemically etched CdTe surfaces. *Appl. Phys. Lett.* **53**(26), 2623–2625 (1988)
 26. I.M. Dharmadasa, J.M. Thornton, R.H. Williams, Effects of surface treatments on Schottky barrier formation at metal/n-CdTe contacts. *Appl. Phys. Lett.* **54**(2), p137 (1989)
 27. M. Ayoub, M. Hage-Ali, A. Zumbiehl, R. Regal, J.M. Koebel, C. Rit, P. Fougères, P. Siffert, *IEEE Trans. Nucl. Sci.* **49**(4), 1954–1959 (2002)
 28. M. Bugár, E. Belas, R. Grill, J. Procházka, S. Uxa, P. Hlidek, J. Franc, R. Fesh, P. Höschl, *IEEE Trans. Nucl. Sci.* **58**(4), 1942–1948 (2011)
 29. M. Ayoub, M. Hage-Ali, J.M. Koebel, A. Zumbiehl, F. Klotz, C. Rit, R. Regal, P. Fougères, P. Siffert, *IEEE Trans. Nucl. Sci.* **50**(2), 229–237 (2003)
 30. J. Hiie, CdTe: CdCl₂:O₂ annealing process. *Thin Solid Films* **431–432**, 90–93 (2003)
 31. M.P.R. Panicker, M. Knaster, F.A. Kröger, Cathodic deposition of CdTe from aqueous electrolytes. *J. Electrochem. Soc.* **125**(4), 566–572 (1978)
 32. D.W. Cunningham, Apollo Thin Film Process Development: Final Technical Report, April 1998–April 2002 (2002), <http://www.nrel.gov/docs/fy03osti/32883.pdf>
 33. M.R. Asabe, V.P. Ubale, A.H. Manikshete, V.T. Vader, S.V. Rajmane, S.D. Delikar, Properties of electrochemically deposited CdTe thin films: annealing effect. *J. Mater. Sci. Mater. Electron.* **24**, 4655–4661 (2013). doi:10.1007/s10854-013-1457-y
 34. I.M. Dharmadasa, A.P. Samantilleke, J. Young, N.B. Chaur, New ways of development of glass/conducting glass/CdS/CdTe/metal thin film solar cells based on a new model. *Semicond. Sci. Technol.* **17**, 1238–1248 (2002)
 35. I.M. Dharmadasa, *Advances in Thin Film Solar Cells* (Pan Stanford Publishing Ltd., Singapore, 2013). **Single authored book**
 36. I.M. Dharmadasa, O.K. Echendu, F. Fauzi, H.I. Salim, N.A. Abdul-Manaf, J.B. Jasinski, A. Sherehiy, G. Sumanasekera, Study of Fermi level movement during CdCl₂ treatment of CdTe thin films using Ultra-violet photoemission spectroscopy. *Mater. Chem. Phys.* (2014)
 37. T. Schulmeyer, J. Fritsche, A. Thißen, A. Klein, W. Jaegermann, M. Campo, J. Beier, Effect of in situ UHV CdCl₂-activation on the electronic properties of CdTe thin film solar cells. *Thin Solid Films* **431–432**, 84–89 (2003)
 38. I.M. Dharmadasa, Third generation multi-layer tandem solar cells for achieving high conversion efficiencies. *Sol. Energy Mater. Sol. Cells* **85**, 293–300 (2005)
 39. I.M. Dharmadasa, J.S. Roberts, G. Hill, Third generation multi-layer graded bandgap solar cells for achieving high conversion efficiencies—II. *Sol. Energy Mater. Sol. Cells* **88**, 413–422 (2005)
 40. J. Britt, C. Ferekides, Thin film CdS/CdTe solar cell with 15.8 % efficiency. *Appl. Phys. Lett.* **62**, 2851–2852 (1993)
 41. X. Wu, J.C. Keane, R.G. Dhere, C. DeHart, D.S. Albin, A. Duda, T.A. Gessert, S. Ashar, D.H. Levi, P. Sheldon, 16.5 %-efficient CdS/CdTe polycrystalline thin film solar cells. In *Proceedings of the 17th European PVSEC*, pp. 995–1000 (2001)